A&A 518, L45 (2010)
DOI: 10.1051/0004-6361/201014530

Astronomy & Astrophysics
Special feature

Herschel: the first science highlights

Letter to the Editor

The dust morphology of the elliptical Galaxy M 86 with SPIRE⋆

H. L. Gomez[1], M. Baes[2], L. Cortese[1], M. W. L. Smith[1], A. Boselli[3], L. Ciesla[3], G. J. Bendo[4], M. Pohlen[1], S. di Serego Alighieri[5], R. Auld[1], M. J. Barlow[6], J. J. Bock[7], M. Bradford[7], V. Buat[3], N. Castro-Rodriguez[8], P. Chanial[9], S. Charlot[10], D. L. Clements[4], A. Cooray[11], D. Cormier[9], J. I. Davies[1], E. Dwek[12], S. Eales[1], D. Elbaz[9], M. Galametz[9], F. Galliano[9], W. K. Gear[1], J. Glenn[13], M. Griffin[1], S. Hony[9], K. G. Isaak[14], L. R. Levenson[7], N. Lu[7], S. Madden[9], B. O'Halloran[3], K. Okumura[9], S. Oliver[15], M. J. Page[16], P. Panuzzo[9], A. Papageorgiou[1], T. J. Parkin[17], I. Perez-Fournon[8], N. Rangwala[13], E. E. Rigby[18], H. Roussel[10], A. Rykala[1], N. Sacchi[19], M. Sauvage[9], M. R. P. Schirm[17], B. Schulz[20], L. Spinoglio[19], S. Srinivasan[10], J. A. Stevens[21], M. Symeonidis[16], M. Trichas[4], M. Vaccari[22], L. Vigroux[10], C. D. Wilson[17], H. Wozniak[23], G. S. Wright[24], and W. W. Zeilinger[25]

(Affiliations are available in the online edition)

Received 29 March 2010 / Accepted 25 April 2010

ABSTRACT

We present *Herschel*-SPIRE observations at 250−500 μm of the giant elliptical galaxy M 86 and examine the distribution of the resolved cold dust emission and its relation with other galactic tracers. The SPIRE images reveal three dust components: emission from the central region; a dust lane extending north-south; and a bright emission feature 10 kpc to the south-east. We estimate that $\sim 10^6$ $M_\odot$ of dust is spatially coincident with atomic and ionized hydrogen, originating from stripped material from the nearby spiral NGC 4438 due to recent tidal interactions with M 86. The gas-to-dust ratio of the cold gas component ranges from ∼20−80. We discuss the different heating mechanisms for the dust features.

Key words. galaxies: ellipticals and lenticular, cD – galaxies: individual: M 86 – submillimeter: ISM – dust, extinction

1. Introduction

Studies of cold dust in elliptical galaxies has been limited to date by the lack of high-resolution, long wavelength spectral coverage. In particular, the origin of far-infrared (FIR) emission in these systems is still a controversial issue, with evidence of dusty disks favouring a stellar origin (e.g. Knapp et al. 1989) and other systems originating from mergers with dust-rich galaxies (Leeuw et al. 2008). The unprecedented resolution and sensitivity of the recently launched *Herschel* Space Observatory (Pilbratt et al. 2010) allows us to address long-standing issues such as the origin and quantity of dust in ellipticals.

One of the most well-known IR-bright ellipticals is the giant Virgo cluster member, M 86, at a distance of 17 Mpc (Mei et al. 2007). Two dust features were detected with IRAS, one coincident with the galaxy and another to the north-west, thought to be coincident with an X-ray plume of gas (Knapp et al. 1989; White et al. 1991) and originally attributed to dust stripped from M 86 due to its motion through the cluster. Higher resolution data from ISO revealed two dust peaks within M 86 suggesting a massive dust complex (Stickel et al. 2003, hereafter S03). They proposed a tidal origin, also supported by absorption features attributed to dust stripped from the nearby dwarf galaxy, VCC 882 (Elmegreen et al. 2000). The discovery of atomic gas offset from the centre of M 86 and decoupled from its stellar disk supports the tidal scenario (Li & van Gorkom 2001). More recently, Kenney et al. (2008, hereafter K08) detected strong Hα features extending from the nearby spiral NGC 4438 at 23′ away, to within 1′ of the nucleus of M 86. The distribution and velocity of the ionized gas provides clear evidence for tidal interaction between these two giants (K08, Fig. 1 Cortese et al. 2010). In this scenario, we are observing debris from the spiral left in the wake of the collision with M 86 with $\sim 10^9$ $M_\odot$ of cold gas removed from NGC 4438 (K08). The stripped material is then heated by the hot interstellar medium (ISM) of M 86 or shock fronts from the interaction. Although tidal stripping from NGC 4438 is supported by the atomic and ionized gas distribution, the origin of the dust responsible for the FIR emission and its heating mechanism is unclear. Here we present submm observations of M 86 with *Herschel*-SPIRE (Griffin et al. 2010). Companion observations of NGC 4438, are presented in Cortese et al. (2010).

2. Observations and data reduction

M 86 was observed with SPIRE at 250, 350 and 500 μm during *Herschel's* science demonstration phase as part of the *Herschel* Reference Survey (Boselli et al. 2010a). Eight pairs of cross-linked observations were taken in scan-map mode with scanning rate 30″/s. The data were processed following the detailed description given in Pohlen et al. (2010) and Bendo et al. (2010a). Calibration methods and accuracies are outlined in Swinyard et al. (2010). The measured 1σ noise level is 5, 6 and 7 mJy beam^{-1} at 250, 350 and 500 μm with beam size 18, 25 and 37″; the noise is dominated by background source confusion.

⋆ *Herschel* is an ESA space observatory with science instruments provided by European-led Principal Investigator consortia and with important participation from NASA.

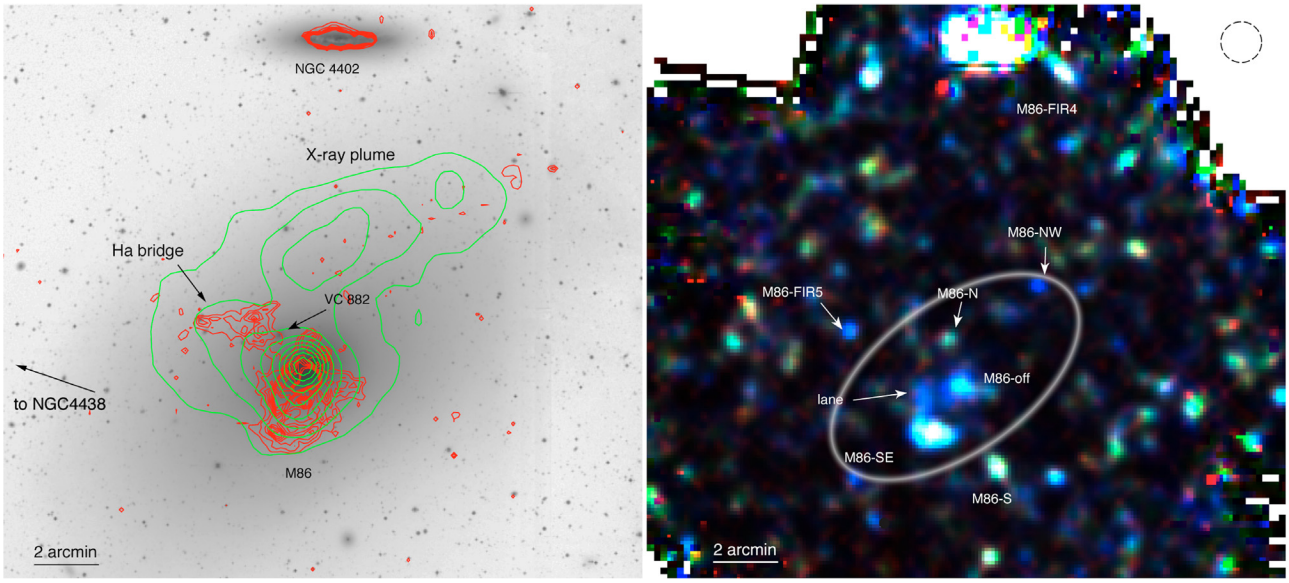

Fig. 1. *Left*: *R*-band image of M 86 region with Hα (red) and X-ray (green) contours. *Right*: three-colour image at 250, 350 and 500 μm, smoothed to 500 μm beam (as indicated by dashed circle in upper right of the figure). The ellipse indicates the optical halo of M 86 (8.9′ × 5.6′).

3. Results

The three-colour SPIRE image is shown in Fig. 1 with dust features labeled (following the terminology of S03) along with an optical image of the same region with X-ray and Hα contours. In the SPIRE image, there are a number of unresolved sources, and at least five extended features. Careful comparison of large scale FUV and IRAS maps of this region show that the cirrus emission is extremely low ruling out a Galactic origin. In Fig. 2, we focus on the central 13′ × 8′ region and compare with structures seen at other wavelengths. Towards the south, M 86-S is coincident with a number of clustered 24 μm sources. In the north-west, the bright source M 86-NW (originally associated with M 86's X-ray plume) has no optical or UV counterpart and peaks at $\lambda < 100\,\mu$m. The bright feature M 86-FIR5 is coincident with an optical galaxy (VPC 463) and, like M 86-FIR4, has a similar flux ratio to M 86-NW. Extending north from M 86, a faint (2−3σ) filament-like submm structure appears to be coincident with blueshifted Hα emission (Fig. 2) attributed to ionized debris from the *incoming* trajectory of the NGC 4438 collision (Trinchieri & di Serego Alighieri 1991; Finoguenov et al. 2004; K08). However, this submm filament is also coincident with a number of distant 24 μm sources. We therefore suggest that this feature along with M 86-S, M 86-NW, M 86-FIR5 and M 86-FIR4 originate from background sources unrelated to M 86.

The submm morphology within the inner 2′ of M 86 is surprisingly complex and differs from the smooth distributions seen in the 24 μm, UV and optical images. We see four distinct features in the SPIRE maps labeled as M 86-N, M 86-off, M 86-SE and "lane" (Fig. 1). M 86-N is a bright unresolved source which is included in the photometry due to its coincidence with a Hα knot in this region[1]. The feature M 86-SE (7.7 × 2.3 kpc) is the brightest feature within the optical halo and is offset from the centre by 1.9′ (10 kpc). To the immediate north of this feature extends the bright "lane" structure. These features are not seen in the *Spitzer* 24 or 70 μm data (although the latter exhibits severe striping effects) but are detected with *ISO* at 90, 135 and 180 μm and *Spitzer* 160 μm (Fig. 2). Although there are four 24 μm point sources coincident with the M 86-SE structure, these are likely to be background sources since corresponding features are not seen in the same position in Hα nor are they coincident with the peaks in the submm emission. These four features (Fig. 2) are spatially coincident with peaks in the redshifted ionized gas (M 86-SE: −120 km s^{-1}, M 86-off: −200−350 km s^{-1}) extending from NGC 4438 (K08) and with atomic HI (Li & van Gorkom 2001). The submm and HI peak in M 86-SE is coincident with an Hα "hole", but this is likely due to the lower resolution of the former. M 86-SE is also contained within an X-ray boundary tracing the X-ray halo (Finoguenov et al. 2004; Randall et al. 2008). The strong spatial correlation between the cool atomic gas, cold dust, ionised gas and hot X-ray boundary shown in Fig. 2 seems to suggest that the dust originates from gas stripped from NGC 4438 and is immersed in the X-Ray halo of M 86.

At first glance, it appears that the "lane" feature and M 86-SE are coincident with dusty filaments seen in absorption (*A* and *B* in Fig. 2; Elmegreen et al. 2000). Careful comparison with the SPIRE images show that their *B* feature is 1.3′ south of M 86-SE, and filament *A* is offset by 0.4′. Faint submm emission is seen at the southern tip of *A* and the atomic gas encompasses feature *B*. We are not able to resolve *A* (at only 6″ across in the optical), but surprisingly we do not detect significant emission associated with *B*. This could be a result of the absorption features arising from foreground dust lanes with low column density, or the dust is simply too cold to be detected with *Herschel*.

3.1. Dust mass and heating within the optical halo

We performed aperture photometry on the IR and submm images from *ISO*, *Spitzer* and SPIRE. The datasets were *wcs*-aligned, and smoothed to the 160 μm beam using the appropriate kernels (Bendo et al. 2010b) and assuming Gaussian beam profiles for SPIRE. Fluxes were measured using two elliptical apertures (Fig. 2) with semi-major, semi-minor axes and position angles of 1.4′×1.0′, 127.5° (encompassing M 86-SE) and 1.0′×1.6′, 31.5° (encompassing M 86-off and M 86-N) respectively. We used an empirical 160 μm PSF to determine the aperture correction (Young et al. 2009). The spectral energy distributions (SEDs) of

[1] We note that M 86-N has similar features to other point sources in the crowded field and could be a background object. It contributes 15% of the flux measured in the aperture for M 86-off.

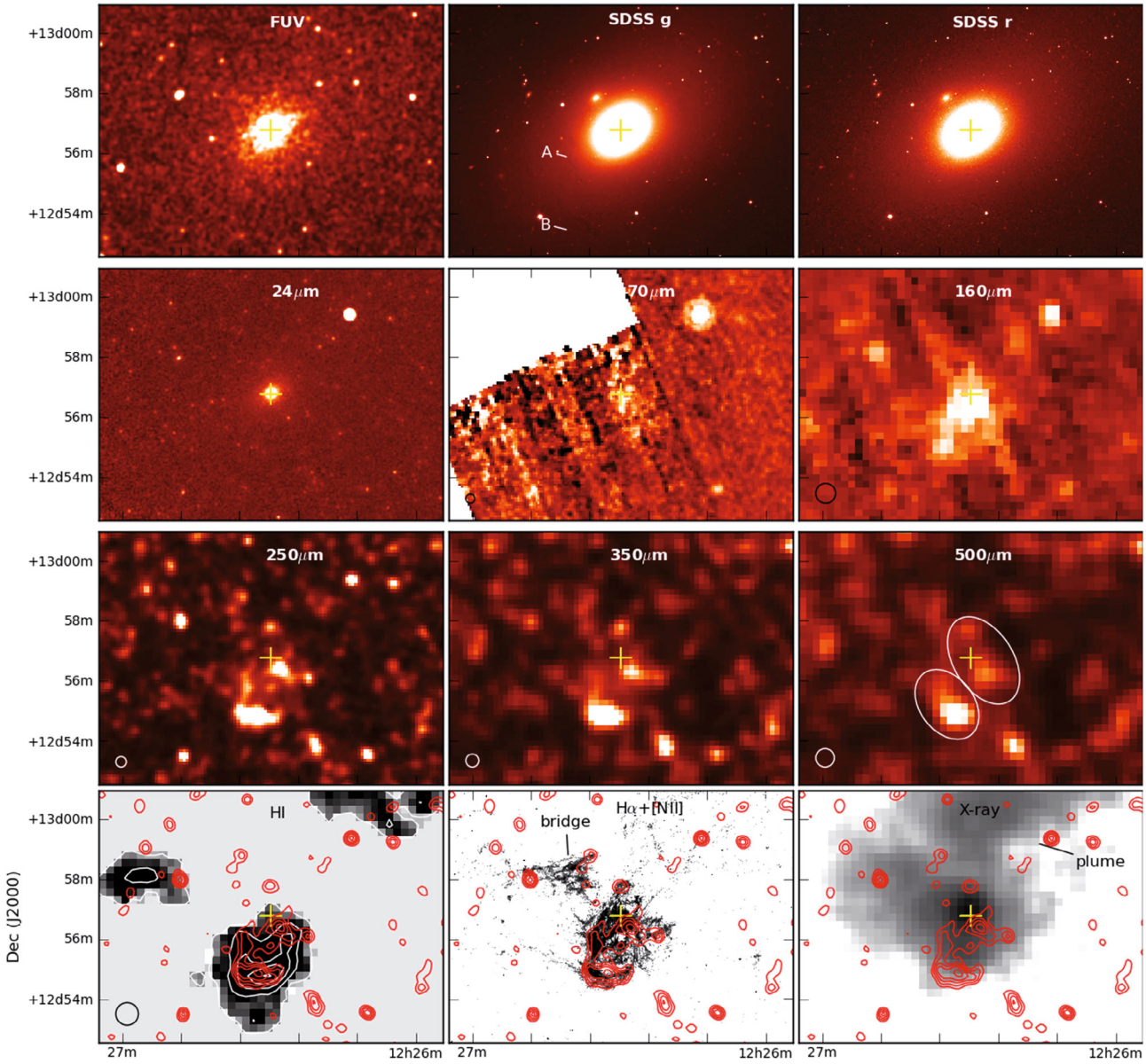

Fig. 2. Multiwavelength comparison of M 86. *Top*: UV (*GALEX*) and optical (SDSS) with absorption features A & B. *Middle*: *Spitzer* 24−160 μm and SPIRE 250−500 μm. White ellipses indicate photometry apertures. *Bottom*: gas emission shown in negative greyscale. HI with white contours 10 + 25 mJy beam^{-1} (courtesy J. van Gorkom). Hα (courtesy J. Kenney) and X-ray (*ROSAT*). 250 μm shown by red contours 9 + 6 mJy beam^{-1}.

M 86-off and M 86-SE are shown in Fig. 3 (see also Boselli et al. 2010b). Blackbody functions modified with a λ^{-2} emissivity law are plotted for comparison with temperatures 15 K and 44 K. Assuming a mass-absorption coefficient, $\kappa_{500} = 0.1\,\mathrm{kg^{-1}\,m^2}$ (Draine 2003), we can estimate a rough dust mass from the total 500 μm flux, S_{500} assuming $M_\mathrm{d} = S_\nu D^2/\kappa_\nu B(\nu, T)$ where D is the distance. The total dust mass within the inner 2′ of M 86 ranges from ∼2−5 × 10^6 $M_\odot$ for temperatures, T_d = 15−20 K. Comparing the dust masses with the atomic gas mass, we estimate a range of gas-to-dust ratios of $g/d \sim 20$−80 depending on the temperature. Non-detection of CO gas within M 86 rules out a significant molecular component with $<10^{6.8}$ $M_\odot$ (Braine et al. 1997). The ionized gas could contribute a further 10^7 $M_\odot$, but this is difficult to estimate without knowing the gas densities (K08). These ratios are higher than expected in elliptical galaxies (e.g. Fich & Hodge 1993) and similar to the lower range of values estimated for the dust feature extending out from NGC 4438 (Cortese et al. 2010).

It is interesting to ask what is responsible for heating the dust and creating the submm emission seen here. Possible mechanisms include AGN, the interstellar radiation field (ISRF), tidal heating and/or the hot X-ray halo. Following Thomas et al. (2002), the luminosity L_h required to heat a cloud of dust with grain size a, total mass M_d, temperature T_d and Planck-averaged absorption coefficient $\langle Q(a, T_\mathrm{d})\rangle$, is given by Eq. (1):

$$L_\mathrm{h} = \left(\frac{4\pi a^2}{m_\mathrm{d}}\right)\langle Q(a, T_\mathrm{d})\rangle T_\mathrm{d}^4 \sigma M_\mathrm{d}. \quad (1)$$

For $a < 0.1\,\mu$m at 20 K, we require $L_\mathrm{h} < 10^9\,L_\odot$. M 86 is radio quiet and we can rule out significant heating from the AGN. Although the dust is not spatially coincident with the optical/UV, the ISRF could still be responsible for heating the dust with L_h comparable to the B-Band luminosity (Mei et al. 2007). To investigate this, we used a radiative transfer implementation of the Monte Carlo code SKIRT (Baes & Dejonghe 2002), which

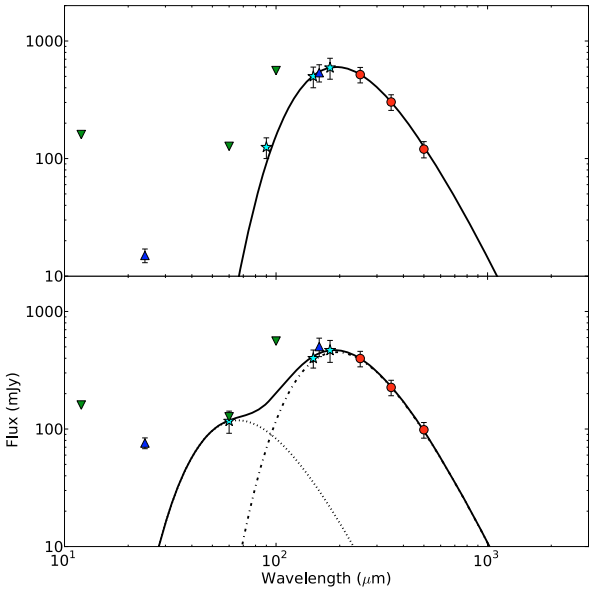

Fig. 3. The SEDs for *top*: M 86-SE and *bottom*: M 86-off. Solid lines are modified blackbody functions with cold temperature 15 K and 44 K. *Spitzer* fluxes are blue triangles, ISO (stars) and SPIRE (circles). IRAS data (green triangles) are measured in a single aperture of radius 136″.

models the absorption, scattering and thermal emission of circumstellar discs and dusty galaxies. M 86 was represented by a flattened Sersic model based on parameters from the literature (Caon et al. 1993; Graham & Colless 1997; Gavazzi et al. 2005) and we used the global SED from Boselli et al. (2010b) for the intrinsic model. During the Monte Carlo simulation, the mean intensity of the radiation field is calculated from UV-MIR wavelengths at every position in the galaxy. From this mean intensity, the equilibrium dust temperature, $T_{\rm eq}$ of each species of dust grains is calculated using energy balance. We predict that $T_{\rm eq}$ for silicate (graphite) grains at a distance of 1.9′ from the nucleus is 13 (19) K; even though the submm peaks do not correlate with optical/UV emission, the ISRF of M 86 is sufficient to produce the submm emission detected here.

The thermal energy provided by M 86's hot, X-ray emitting ISM could also provide a significant heating contribution by collisionally heating the dust, with grains of $a < 0.1\,\mu$m reaching $T_{\rm eq} < 18$ K (e.g. Dwek 1987). The tidally-heated component as traced by Hα also cannot be ruled out as it provides comparable energy to M 86's thermal reservoir over the last 100 Myr ($\sim 10^9\,L_\odot$, K08). Thus, the ISRF, X-ray halo and tidal heating could all be contributing to heating the dust and it is difficult to separate these processes using the UV-submm SED only. However, the high resolution images presented here suggest that submm emission only originates from regions where we detect atomic *and* ionised gas. Submm emission is not detected from regions with just atomic HI and X-ray emission, suggesting that the X-ray halo alone is not responsible for heating the dust. The spatial distribution of these tracers therefore favours a scenario in which the submm emission originates from dust mixed with stripped atomic material and is heated by the tidal interaction.

In summary, we present submm images of M 86 which reveal a complex dust morphology with emission detected 10 kpc from the centre, towards the southeast. The unprecedented resolution of SPIRE has revealed, for the first time, a strong spatial correlation between the cold dust ($\sim 10^6\,M_\odot$, g/d of 20−80) and the warm ionized gas in M 86. This result strongly favours a scenario whereby the dust in M 86 originates from material stripped from the nearby spiral NGC 4438. We investigate the different heating mechanisms responsible for the dust emission detected by *Herschel*. Intriguingly, although we cannot rule out the stellar radiation field of M 86, the strong correlation between submm and Hα emission suggests the cold dust is heated by the same mechanisms responsible for ionizing the gas stripped from NGC 4438. If so, tidal heating is likely to be responsible for the dust emission. Further modeling is required to provide a definite answer on the origin of the submm features revealed by SPIRE in M 86.

Acknowledgements. We thank Jeff Kenney & Jacqueline van Gorkom for providing electronic versions of their data. The images were produced with APLpy, thanks to Edward Gomez & Eli Bressart. We thank the referee for their constructive comments. SPIRE has been developed by a consortium of institutes led by Cardiff University (UK) and including Univ. Lethbridge (Canada); NAOC (China); CEA, OAMP (France); IFSI, Univ. Padua (Italy); IAC (Spain); Stockholm Observatory (Sweden); Imperial College London, RAL, UCL-MSSL, UKATC, Univ. Sussex (UK); and Caltech/JPL, IPAC, Univ. Colorado (USA). This development has been supported by national funding agencies: CSA (Canada); NAOC (China); CEA, CNES, CNRS (France); ASI (Italy); MCINN (Spain); Stockholm Observatory (Sweden); STFC (UK); and NASA (USA).

References

Baes, M., & Dejonghe, H. 2002, MNRAS, 335, 441
Boselli, A., Eales, S., Cortese, L., et al. 2010a, PASP, 122, 261
Boselli, A., Ciesla, L., Buat, V., et al. 2010b, A&A, 518, L61
Braine, J., Henkel, C., & Wiklind, T. 1997, A&A, 321, 765
Bendo, G. J., et al. 2010a, A&A, 518, L65
Bendo, G. J., Wilson, C. D., Warren, B. E., et al. 2010b, MNRAS, 402, 1409
Caon, N., Capaccioli, M., & D'Onofrio, M. 1993, MNRAS, 265, 1013
Cortese, L., Bendo, G. J., Boselli, A., et al. 2010, A&A, 518, L63
Draine, B. T. 2003, Ann. Rev. Astr. Ap., 41, 241
Dwek, E. 1987, ApJ, 332, 812
Elmegreen, D. M., Elmegreen, B. G., Chromey, F. R., & Fine, M. S. 2000, ApJ, 120, 733
Fich, M., & Hodge, P. 1993, ApJ, 415, 75
Finoguenov, A., Pietsch, W., Aschenbach, B., & Miniati, F. 2004, A&A, 415, 415
Gavazzi, G., Donati, A., Cucciati, O., et al. 2005, A&A, 430, 411
Graham, A., & Colless, M. 1997, MNRAS, 287, 221
Griffin, M. J., et al. 2010, A&A, 518, L3
Kenney, J. D. P., Tal, T., Crowl, H. H., Feldmeier, J., & Jacoby, G. H. 2008, ApJ, 687, L69 [K08]
Knapp, G. R., Guhathakurta, P., Kim, D.-W., & Jura, M. A. 1989, ApJS, 70, 329
Mei, S., Blakeslee, J. P., Côté, P., et al. 2007, ApJ, 655, 144
Leeuw, L. L., Davidson, J., Dowell, C. D., & Matthews, H. E. 2008, ApJ, 677, 249
Li, Y., & van Gorkom, J. H. 2001, in Gas and Galaxy Evolution, ed. J. E. Hibbard, M. Rupen, & J. H. van Gorkom, ASP Conf. Ser., 240, 637
Pilbratt, G. L., et al. 2010, A&A, 518, L1
Pohlen, M., Cortese, L., Smith, M. W. L., et al. 2010, A&A, 518, L72
Randall, S., Nulsen, P., Forman, W. R., et al. 2008, ApJ, 688, 208
Stickel, M., Bregman, J. N., Fabian, A. C., White, D. A., & Elmegreen, D. M. 2003, A&A, 397, 503 [S03]
Swinyard, B. M., et al. 2010, A&A, 518, L4
Thomas, H. C., Dunne, L., Clemens, M. S., et al. 2002, MNRAS, 331, 853
Trinchieri, G., & di Serego Alighieri, S. 1991, AJ, 101, 1647
Young, L. M., Bendo, G. J., & Lucero, D. M. 2009, AJ, 137, 2
White, D. A., Fabian, A. C., Forman, W., Jones, C., & Stern, C. 1991, ApJ, 375, 35

[1] School of Physics & Astronomy, Cardiff University, The Parade, Cardiff, CF24 3AA, UK
e-mail: haley.gomez@astro.cf.ac.uk
[2] Sterrenkundig Observatorium, Universiteit Gent, Krijgslaan 281 S9, 9000 Gent, Belgium
[3] Astrophysics Group, Imperial College, Blackett Laboratory, Prince Consort Road, London SW7 2AZ, UK
[4] Laboratoire d'Astrophysique de Marseille, UMR6110 CNRS, 38 rue F. Joliot-Curie, 13388 Marseille, France
[5] INAF-Osservatorio Astrofisico di Arcetri, Largo E. Fermi 5, 50125 Firenze, Italy
[6] Dept. of Physics and Astronomy, University College London, Gower Street, London WC1E 6BT, UK
[7] Jet Propulsion Laboratory, Pasadena, CA 91109, California Institute of Technology, Pasadena, CA 91125, USA
[8] Instituto de Astrofísica de Canarias (IAC) and Departamento de Astrofísica, Universidad de La Laguna (ULL), La Laguna, Tenerife, Spain
[9] CEA, Laboratoire AIM, Irfu/SAp, Orme des Merisiers, 91191 Gif-sur-Yvette, France
[10] Institut d'Astrophysique de Paris, UMR7095 CNRS, 98 bis Boulevard Arago, 75014 Paris, France
[11] Dept. of Physics & Astronomy, University of California, Irvine, CA 92697, USA
[12] Observational Cosmology Lab, Code 665, NASA Goddard Space Flight Center Greenbelt, MD 20771, USA
[13] Department of Astrophysical and Planetary Sciences, CASA CB-389, University of Colorado, Boulder, CO 80309, US
[14] ESA Astrophysics Missions Division, ESTEC, PO Box 299, 2200 AG Noordwijk, The Netherlands
[15] Astronomy Centre, Department of Physics and Astronomy, University of Sussex, UK
[16] Mullard Space Science Laboratory, University College London, Holmbury St Mary, Dorking, Surrey RH5 6NT, UK
[17] Dept. of Physics & Astronomy, McMaster University, Hamilton, Ontario, L8S 4M1, Canada
[18] School of Physics & Astronomy, University of Nottingham, University Park, Nottingham NG7 2RD, UK
[19] Istituto di Fisica dello Spazio Interplanetario, INAF, via del Fosso del Cavaliere 100, 00133 Roma, Italy
[20] Infrared Processing and Analysis Center, California Institute of Technology, 770 South Wilson Av, Pasadena, CA 91125, USA
[21] Centre for Astrophysics Research, Science and Technology Research Centre, University of Hertfordshire, Herts AL10 9AB, UK
[22] University of Padova, Department of Astronomy, Vicolo Osservatorio 3, 35122 Padova, Italy
[23] Observatoire Astronomique de Strasbourg, UMR 7550 Université de Strasbourg - CNRS, 11, rue de l'Université, 67000 Strasbourg, France
[24] UK Astronomy Technology Center, Royal Observatory Edinburgh, Edinburgh, EH9 3HJ, UK
[25] Institut für Astronomie, Universität Wien, Türkenschanzstr. 17, 1180 Wien, Austria